Colloid Polym Sci (2014) 292:1111–1120
DOI 10.1007/s00396-013-3151-2

ORIGINAL CONTRIBUTION

Micellization behavior of the ionic liquid lauryl isoquinolinium bromide in aqueous solution

Xiaohong Zhang · Xinying Peng · Lingling Ge · Lei Yu · Zhimin Liu · Rong Guo

Received: 12 April 2013 / Revised: 19 November 2013 / Accepted: 25 December 2013 / Published online: 18 January 2014

Abstract The micellization behavior of the ionic liquid lauryl isoquinolinium bromide ([C_{12}iQuin]Br) in aqueous solution has been assessed using surface tension, electrical conductivity, and ^{1}H nuclear magnetic resonance (NMR) measurements. The results reveal that the critical micelle concentration (CMC) and constant surfactant tension (γ_{cac}) are lower than that of butyl isoquinolinium bromide ([C_4iQuin]Br), octyl isoquinolinium bromide ([C_8iQuin]Br, and lauryl pyridinium bromide ([C_{12}Pyr]Br). ^{1}H NMR spectra show the evidence of paralleled π-stacking of adjacent isoquinoline rings. To elucidate the effect of the π–π interactions on the aggregation process, thermodynamic parameters such as the standard free energy, enthalpy, and entropy of aggregation have been discussed. These parameters are evaluated from the CMC with temperature by fitting these values to expressions derived from a micellization thermodynamic model. The enthalpy–entropy compensation phenomenon has been observed in the micellization process of [C_{12}iQuin]Br in water, and the presence of isoquinoline cations is responsible for the decrease in the ΔH^*_{mic}, compared with [C_{12}Pyr]Br which has the same alkyl chain and counter-ion.

Keywords Isoquinoline · Ionic liquids · Micellar properties · π-Stacking · Enthalpy–entropy compensation

Introduction

Ionic liquids (ILs) are salt-substances composed essentially of ions—exhibiting a melting point below a conventional temperature of 100 °C. ILs are formed by ions, with at least one of the constituent ions as organic, and the cations and anions differ significantly in their geometrical characteristics. ILs that are inherently amphiphilic are called surface active ionic liquids (SAILs) or IL-based surfactants, a type of functional ILs with combined properties of ILs and surfactants [1]. It is stilled argued that the cation–anion pair no longer constitutes a true ionic liquid when SAILs are dissolved in solvents. Therefore, the self-aggregation behavior of SAILs in aqueous solution has generated interest. In addition, it is also worthful to compare the properties of SAIL solutions and hence their applications with those of "conventional" surfactants in the colloid and interface field [2–7] since the first work by Bowers et al. in 2004 [8]. What is more, it is known that the ability to modify the properties of the aggregate formation by easily changing the structural make-up of the cation–anion pair draws obvious parallels to the tunability of classic ionic liquids. In addition, the conformation of surfactant in micelle also influences the important parameters of regioselectivity [9], reaction kinetics [10], and enantioselectivity [11]. The aggregation character of ILs in solutions will affect their application in chemical synthesis, catalysis, electrochemistry, extraction, and chromatography, as well as in the synthesis of new materials. In fact, the variety of possible SAILs that can be synthesized has the potential to make a huge impact in the field of surfactant development and design, particularly with respect to traditional cationic surfactants. Pyridinium-based ionic liquids are an important class of cations in the SAILs family, and their aggregation has been thoroughly investigated in aqueous solutions [12–15]. Isoquinoline contains a pyridine ring fused to a benzene ring. Isoquinolinium compounds are also valuable biologically active chemical substances in the

Electronic supplementary material The online version of this article (doi:10.1007/s00396-013-3151-2) contains supplementary material, which is available to authorized users.

X. Zhang · X. Peng · L. Ge · L. Yu · Z. Liu · R. Guo (✉)
School of Chemistry and Chemical Engineering, Yangzhou University, Yangzhou, People's Republic of China
e-mail: guorong@yzu.edu.cn

medical field [16]. Isoquinolinium-based ionic liquids were rarely investigated [17] though the hydrophobic isoquinolinium ionic liquids have been recognized and successfully applied in liquid–liquid separations for 10 years [18]. Recently, Domańska and co-workers [19–22] reported the phase equilibria diagrams, volumetric and transport properties, and activity coefficients at infinite dilution of diverse organic solutes for *N*-alkylisoquinolinium bis (trifluoromethylsulfonyl) imides homologous series ([C_niQuin][NTf_2], where $C_n \equiv C_nH_{2n+1}$ and n=4, 6, and 8). But no aggregation behavior in water has been reported for these ionic liquids, though *N*-alkylisoquinolinium bromides with an alkyl chain up to dococyl have been synthetized. Lauryl isoquinolinium bromide (abbreviated in present work by [C_{12}iQuin]Br) is a solid at room temperature with a lower melting point (~49 °C) and is a type of cationic surfactant. Therefore, [C_{12}iQuin]Br can also be considered a SAILs. The results of preliminary experiments show that [C_{12}iQuin]Br exhibit more antimicrobial activity than quaternary ammonium-based surfactants and pyridinium ILs possessing the same alkyl chain and counter-ion. It is obvious that their antimicrobial activity is closely related to their structure of head group and the related association phenomena in solutions. The purpose of this study is to characterize the thermodynamics of the micellization of [C_{12}iQuin]Br and the micellar structure. To better understand of the role of cation playing on micellization, the physicochemical properties of the aqueous [C_{12}iQuin]Br solution will be compared with that reported data for 1-dodecylpyridinium bromide ([C_{12}Pyr]Br), which has the same alkyl chain length and counter-ion. In addition, the shorter length alkyl chain isoquinolinium-based ionic liquids, butyl isoquinolinium bromide ([C_4iQuin]Br), and octyl isoquinolinium bromide ([C_8iQuin]Br) were prepared in order to study the effect of alkyl chain length on micellization of isoquinolinium-based SAILs. This goal is achieved by using surface tension, electrical conductivity, and ^{1}H nuclear magnetic resonance (NMR) measurements.

Experimental section

Materials

Isoquinoline was purchased from Hatch Chemical Co., Ltd. of China. 1-Bromobutane (99 %), 1-bromooctane (99 %), and 1-bromododecane (99 %), anhydrous ether, petroleum ether, and methylene chloride were obtained from Sinopharm Chemical Reagent Co., Ltd, of China and were used without further purifications. D_2O was obtained from Beijing Chemical Factory of China and was 99.8 % deuterated. All aqueous solutions were prepared with Millipore grade water.

Synthesis

A certain amount of isoquinoline and alkyl bromide were added successively to a 50-mL round flask under nitrogen atmosphere. The mixture was heated to reflux and maintained 2 h. The crude product was dissolved by DCM and decolorized by activated carbon, and a thick red oil was obtained. After washing three times with petroleum ether, a white solid was obtained. Further recrystallization with methanol afforded the pure [C_niQuin]Br (n=4, 8, 12).

Methods

Aqueous solutions of [C_niQuin]Br were prepared by weight using an analytical balance with a precision of ±0.0001 g (Denver Instrument APX-200). The surface tension of aqueous solutions was measured by a Tensiometer (Dataphysics, Germany, Model DCAT 11) using the Wilhelmy plate method. The measured surface tension has an uncertainty of ±0.02 mN m^{-1}. The temperature was controlled using a constant temperature circulating water thermostat bath at 25±0.1 °C. The electrical conductivity of the solution was measured by a digital conductivity meter (Lei Ci, China, Model DDS-11) using a cell with platinized platinum electrodes. The cell was calibrated with aqueous KCl solutions in the concentration range of 0.01–1.0 mol L^{-1}. At least three measurements were made for each concentration, and the mean values were taken into analysis consideration. The uncertainty of the measurements was less than 0.2 %. Each sample was placed in a cell within a thermostat bath at temperatures ranging from 15 to 45 °C (±0.1 °C).

The ^{1}H NMR spectra of [C_niQuin]Br solutions prepared in D_2O were taken at 25 °C on an AVANCE 600 NMR spectrometer (Bruker, Germany). The acquisition of spectra and its analysis was handled by TOPSPIN-13 software provided by the supplier. The proton chemical shifts were referenced with respect to an external standard DSS (δ=0.000 ppm) in D_2O. The chemical shifts of the peaks of interest were determined using Mestre Nova 8.0 software. Two-dimensional nuclear Overhauser enhancement spectroscopy (2D NOESY) experiments were performed with the standard three-pulse sequence with mixing time of 350 ms for [C_niQuin]Br solution.

Results and discussion

Surface absorption and micellization of [C_{12}iQuin]Br

Surface tension measurements The surface tension was measured to evaluate the surface activity of the aqueous [C_{12}iQuin]Br solutions. Figure 1 shows the plot of surface tension as a function of the logarithmic concentration obtained

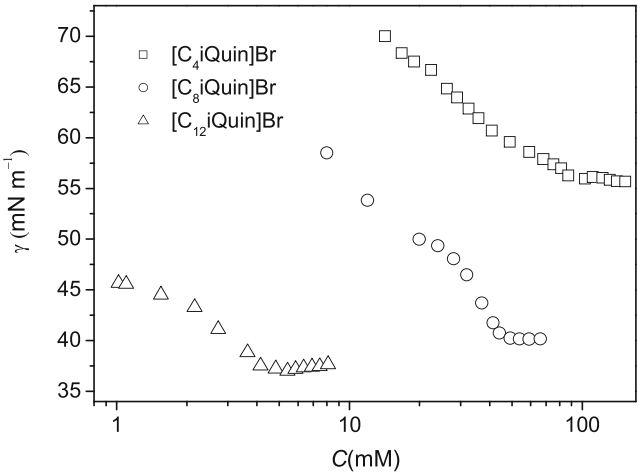

Fig. 1 Surface tension isotherms for [C_4iQuin]Br, [C_8iQuin]Br, and [C_{12}iQuin]Br aqueous solutions at 298 K

for [C_{12}iQuin]Br aqueous solutions at 298 K. As dearly demonstrated, the surface tension of the aqueous phase showed a progressive decrease with increasing ILs concentration and remained constant above the critical concentration. The concentration at the break point corresponding to the critical micelle concentration (CMC) and the value of constant surface tension (γ_{CMC}) are all summarized in Table 1. The relative Gibbs surface excess of the saturated [C_{12}iQuin]Br monolayer at the air/solution interface, Γ_{max}, was calculated from the slope of the linear profile of the tensiometric isotherm up to the CMC according to the standard Gibbs adsorption equation [23]. The area of exclusion per monomer (A_{min}) was obtained by $A_{min}=1/(N_A\Gamma_{max})$, where N_A is the Avogadro constant (6.022×10^{23} M^{-1}).

Comparing with 1-dodecylpyridinium bromide ([C_{12}Pyr]Br), it can been found that the ability and the efficiency of [C_{12}iQuin]Br to decrease surface tension are superior to [C_{12}Pyr]Br [12]. This is mainly because isoquinoline contains a pyridine ring fused to a benzene ring and certainly prefers the formation of π-stacking due to the conjugation effect.

The surface tension isotherms of [C_4iQuin]Br and [C_8iQuin]Br are also shown in Fig. 1, and the CMC, γ_{cac}, A_{min} are listed in Table 1, respectively, for comparison. The values in Table 1 show clearly that the CMC and γ_{cac} values decrease with the increase of alkyl chain length, which indicates that the surface activity of [C_{12}iQuin]Br is superior to both of [C_4iQuin]Br and [C_8iQuin]Br.

Nuclear magnetic resonance measurements As a sensitive and accurate technique, ^{1}H NMR was widely used to investigate the aggregation behavior of SAILs [24–26]. The different protons as numbered in the chemical structure of [C_{12}iQuin]Br are shown in Fig. 6, and a summary of the ^{1}H NMR-observed chemical shifts (δ_{obsd}) for distinguishable protons of [C_{12}iQuin]Br at different concentrations is supplied in Supporting Information (Table S1). With the help of the pseudo-phase mode of micellization, the δ_{obsd} of the terminal methyl group in the alkyl chain has been used to determine the CMC under fast exchange in the NMR time scale in bulk solution [25]. Figure 2 shows the δ_{obsd} values for terminal CH_3 versus the reciprocal concentration for [C_{12}iQuin]Br. As expected, the plot of δ_{obsd} versus C^{-1} can be linearly fit by two straight lines. The break point provides concentrations corresponding to CMC. The plots of δ_{obsd} versus C^{-1} of [C_4iQuin]Br and [C_8iQuin]Br are shown in the inset of Fig. 2 for comparison. The CMC values obtained from the ^{1}H NMR data are listed in Table 1, which are a bit smaller than the value determined by the surface tension measurement, because the micelles formed in D_2O are more structured than H_2O, as the hydrogen bond network formed in D_2O is stronger than that in H_2O [27].

According to the single-step equilibrium model and based on the mass-action law of micelle formation, the variation of chemical shifts of [C_{12}iQuin]Br protons in aqueous solution can be employed to determine the aggregation number. The principle of calculation has been discussed in details in [25, 26]; thus, only the essentials will be given here in Eq. (1).

$$\log(C_t|\delta_{mon}-\delta_{obsd}|) = N\log(C_t|\delta_{obsd}-\delta_m|) + \log(NK) + (1-N)\log|\delta_{mon}-\delta_m| \quad (1)$$

Table 1 Micellization parameters for [C_niQuin]Br (n=4, 8, 12) in aqueous solution obtained by different techniques at 298 K

ILs	Surface tension			Conductivity			NMR
	CMC (mM)	γ_{CMC} (mN m^{-1})	A_{min} (nm^2)	CMC (mM)	β	ΔG^0_{mic} (kJ M^{-1})	CMC (mM)
[C_4iQuin]Br	86.7	56.1	0.99	85.4	0.42	−22.8	80.3
[C_8iQuin]Br	46.3	40.5	0.59	46.5	0.34	−23.5	45.5
[C_{12}iQuin]Br	4.0	37.9	0.68	4.9	0.64	−38.0	3.6
[C_{12}Pyr]Br*	9.3	39.3	0.71	12	0.74	−36.4	9.3

*[12]

The reported values of [C_{12}Pyr]Br are also shown for comparison

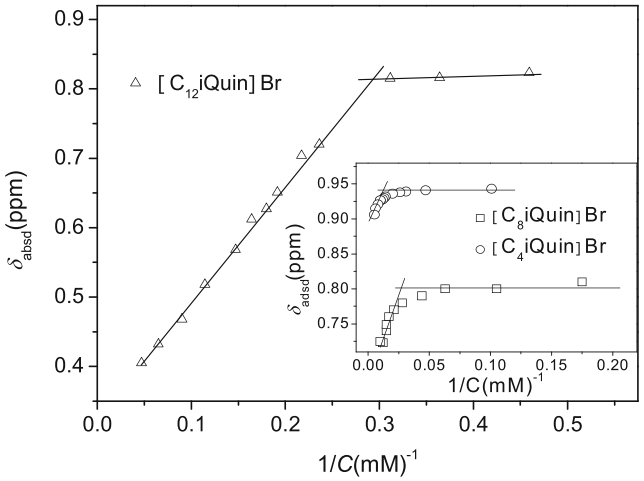

Fig. 2 Variation of δ_{obsd} for the proton of the terminal carbon of [C_4iQuin]Br, [C_8iQuin]Br, and [C_{12}iQuin]Br against the reciprocal concentration, respectively, at 298 K

where N is the aggregation number; K is an equilibrium constant, $K=[A_N]/[A]$, A and A_N are the monomeric and aggregated forms of SAILs; C_t is the total SAILs concentration; and δ_{mon} and δ_m can be determined by extrapolation of the plots of δ_{obsd} versus C_T and δ_{obsd} versus C_T^{-1}. Figure 3 shows the chemical shift data plotted according to Eq. (1) for [C_{12}iQuin]Br in D_2O, where shows two straight lines. The concentration at the point of intersection corresponds to the CMC of [C_{12}iQuin]Br which is in agreement with that obtained from Fig. 2. The slopes of the linear fragments above and below CMC are the values of the aggregation numbers, respectively. The calculated aggregation number is 56 above CMC. It should be mentioned that the value obtained below CMC is lesser than 1, which is reasonable, since [C_{12}iQuin]Br exists as single monomer.

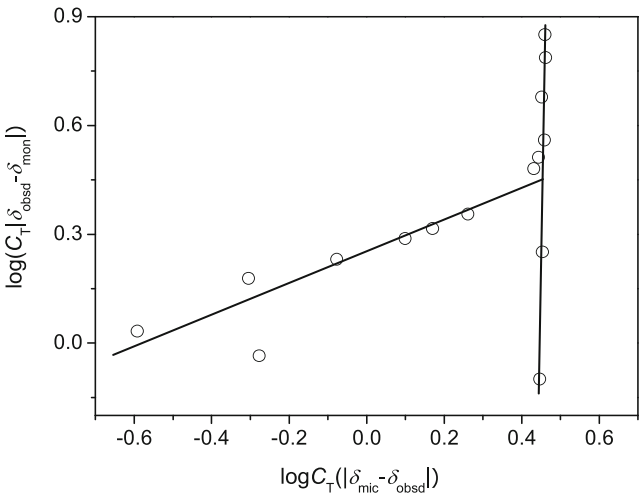

Fig. 3 NMR chemical data plotted in terms of Eq. (1) for [C_{12}iQuin]Br

Conductivity measurements The specific conductivity (κ) results proved thermodynamic information regarding the onset of the aggregation process and the degree of counter-ion binding (β). Figure 4a depicts the change of the κ as a function of concentration of the [C_{12}iQuin]Br solutions in the temperature range of 288–318 K. The specific conductivity values were fit into two straight lines with different slopes. The intersect at the concentration corresponds to the micelle formation which allows for the identification of the CMC [28]. As shown in Table 1, the CMC value obtained from conductivity measurement is similar to the result from tensiometry at 298 K. The change of slope obtained in Fig. 4 was assigned to the onset of micellization due to the decrease of free charged species in the bulk and a lower mobility extent of micelle than the free ions. The value of counter-ion dissociation degree (α), determined by Frahm's method (i.e., as the ratio of the slopes of the linear fragments above and below CMC [29]) and counter-ion binding degree to micelles (β), is equal to $1-\alpha$. According to the charged phase separation model of

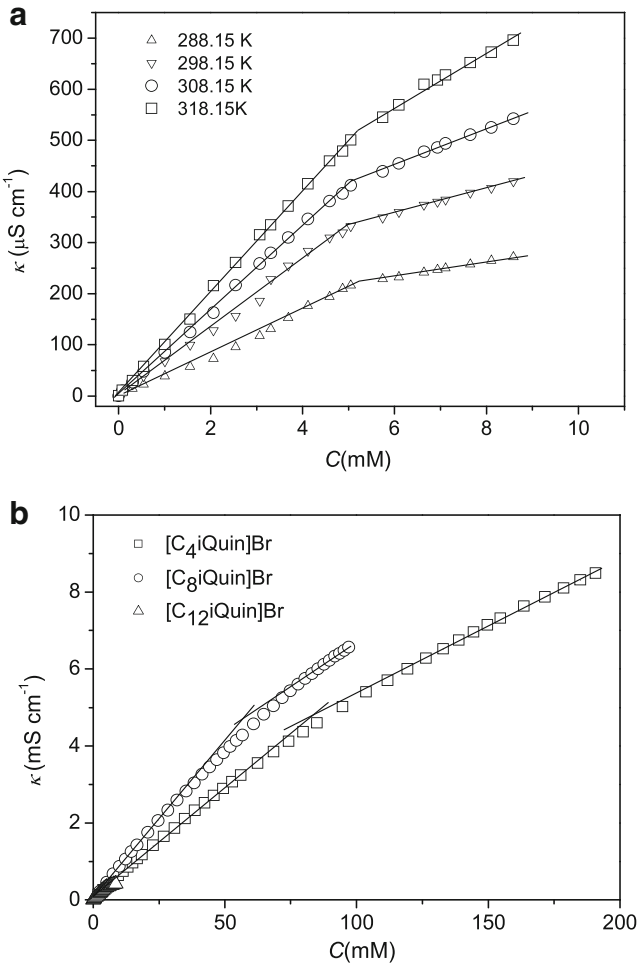

Fig. 4 Plot of electrical conductivity versus the concentration of [C_{12}iQuin]Br at different temperatures (**a**) and [C_niQuin]Br (n=4, 8, 12) at 298 K (**b**)

Table 2 Critical micelle concentration, degree of counter-ion binding to micelle (β), and standard thermodynamic parameters of micellization of [C_{12}iQuin]Br at different temperatures using conductivity measurement

ILs	Temperature (K)	CMC (mM)	β	ΔG^0_{mic} (kJ M^{-1})	ΔH^0_{mic} (kJ M^{-1})	$-T\Delta S^0_{mic}$ (kJ M^{-1})
[C_{12}iQuin]Br	288	5.1	0.68	−37.32	−10.23	−27.95
[C_{12}iQuin]Br	298	4.9	0.64	−37.95	−34.93	−3.02
[C_{12}iQuin]Br	308.	5.1	0.52	−37.63	−58.02	20.40
[C_{12}iQuin]Br	318	5.2	0.50	−36.65	−79.67	43.01

CMC critical micelle concentration

micellization [30], the standard Gibbs energy of aggregation, ΔG^0_{mic}, can be calculated from the following relation:

$$\Delta G^0_{mic} = (1+\beta)TR\ln x_{CMC} \quad (2)$$

where x_{CMC} is the CMC expressed as the mole fraction. The values of CMC and ΔG^0_{mic} in the temperature range of 288–318 K are included in Table 2.

Compared with [C_{12}Pyr]Br [12], [C_{12}iQuin]Br has a much lower β value. From a chemical structure point of view, it is probably due to the larger size of the isoquinoline ring compared with the pyridine ring, which results in an attenuation of the interaction between the Br^- and hydrophilic group. In addition, [C_{12}iQuin]Br has a more negative ΔG^0_{mic} compared with [C_{12}Pyr]Br, which suggests that [C_{12}iQuin]Br is more favorable to aggregate.

Compared with the conductivity measurements of [C_4iQuin]Br and [C_8iQuin]Br aqueous solutions (Fig. 4b; Table 1), [C_{12}iQuin]Br has a higher β, which means a denser arrangement of [C_{12}iQuin]Br molecules at the micellar interface compared with those of short chain [C_niQuin]Br. It can be seen that the longer the alkyl chain of [C_niQuin]Br, the more negative the ΔG^0_{mic}, indicating that the micellization comes more easily with the increase of the alkyl chain length of [C_niQuin]Br.

Furthermore, the enthalpy and entropy of micellization, ΔH^0_{mic} and $-T\Delta S^0_{mic}$, determined from the temperature dependence of the Gibbs energy have been calculated by using the van't Hoff equation and the Gibbs–Helmholtz equation, respectively [31], and the results are shown in Table 2 and Fig. S1. The effect of π-stacking interactions between the adjacent groups may be the fundamental reason for the large negative ΔH^0_{mic} at high temperatures, similar to the case for long-chain *N*-aryl-imidazolium ionic liquids [32]. $T\Delta S^0_{mic}$ and ΔH^0_{mic} dominate ΔG^0_{mic} at lower temperature. A cross-point in temperature appears due to the significant increase of $-T\Delta S^0_{mic}$ and decrease of ΔH^0_{mic} with the increase in temperature. Such changes compensate for each other, resulting in relatively constant Gibbs free energy value. This phenomenon is known as enthalpy–entropy compensation. Figure 5 shows the enthalpy–entropy compensation plots which can be described by the linear relationship [33–35]:

$$\Delta H^0_{mic} = \Delta H^*_{mic} + T_c\Delta S^0_{mic} \quad (3)$$

where T_c is the compensation temperature which has been proposed as a measurement of the desolvation in the process of aggregation [36]. The intercept ΔH^*_{mic} is the enthalpy change at a specific temperature given that $\Delta S^0_{mic}=0$ [37] which means that the driving force for the micelle formation comes only from the enthalpy term. The steadier the structure of the micelle, the larger is the negative value of ΔH^*_{mic}. By fitting the experimental data, shown in Fig. 5, the values for T_c and ΔH^*_{mic} have been obtained as 302 K and −38 kJ M^{-1}, respectively. The enthalpy–entropy compensation relation for micellar formation of [C_{12}Pyr]Br is plotted based on [38]. Both [C_{12}iQuin]Br and [C_{12}Pyr]Br have practically the same compensation temperature ([C_{12}Pyr]Br, T_c=301 K) [38]. This result indicates that the de-solvation process of micellization exhibits a very similar characteristic for both surfactants. The ΔH^*_{mic} value of [C_{12}iQuin]Br is lower than that of [C_{12}Pyr]Br (ΔH^*_{mic}=−21.3 kJ M^{-1}) [35, 38]. It is known that the stronger

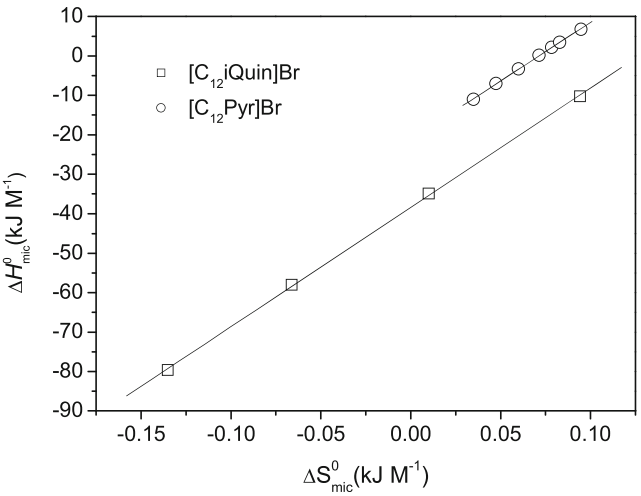

Fig. 5 Enthalpy–entropy compensation relation for micellar formation of [C_{12}iQuin]Br and [C_{12}Pyr]Br [31] in water

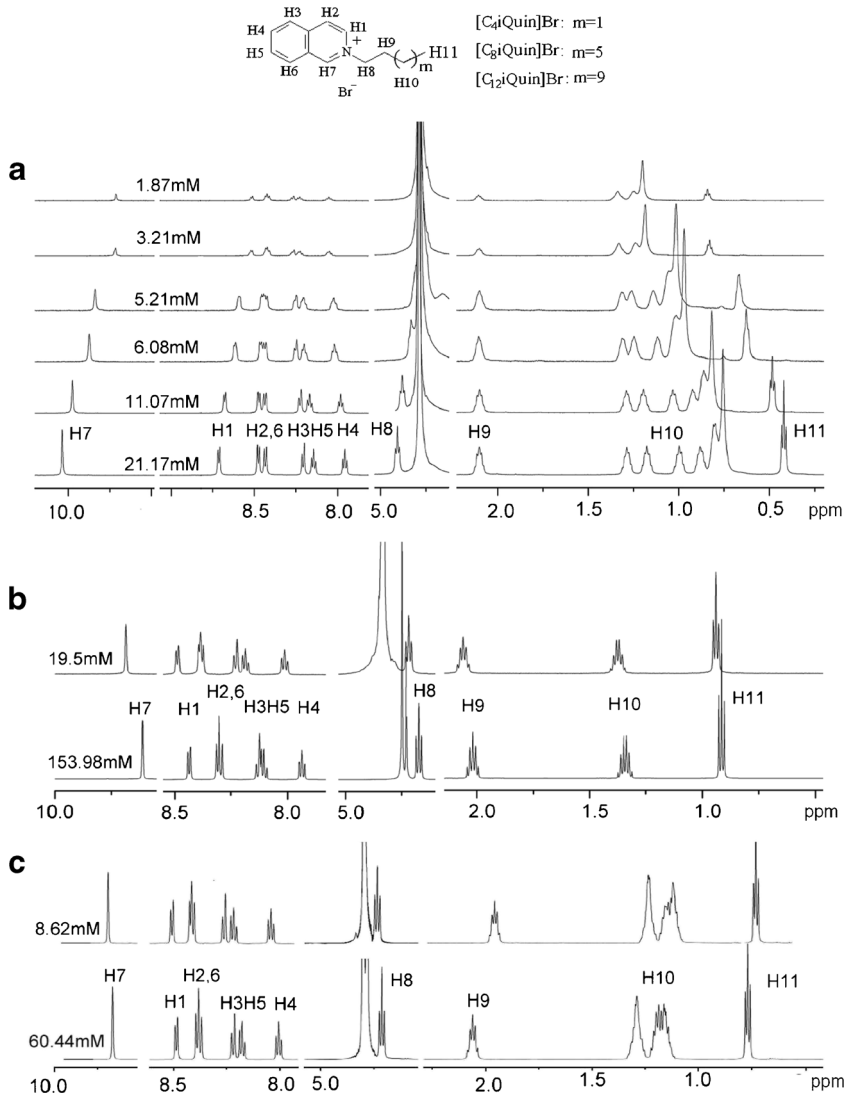

Fig. 6 Parts of the 600-MHz ^{1}H NMR spectra and proton assignments of [C_{12}iQuin]Br (**a**), [C_4iQuin]Br (**b**), and [C_8iQuin]Br (**c**) at 298 K in D_2O

the hydrophobicity, the larger is the negative value of ΔH^*_{mic}. We can safely concluded that the [C_{12}iQuin]Br micelle is stable than that of [C_{12}Pyr]Br due to the dramatic difference in the tendency of the stack of isoquinoline rings and pyridine rings.

The orientation of aromatic ring and alkyl chain in the formation of [C_{12}iQuin]Br micelle

The changes in ^{1}H NMR spectra with the surfactant concentration can shed light on the intermolecular interactions and also on the conformational changes of SAIL aggregation process. Figure 6a shows representative expanded peaks of [C_{12}iQuin]Br protons below and above CMC in D_2O. The variation of the chemical shift, $\Delta\delta_{obsd}$ (= $\delta_{obsd}-\delta_{mon}$), as a function of the concentration of [C_{12}iQuin]Br is presented in Fig. 7. The chemical shifts of all signals are identical below CMC, whereas above CMC, the resonances experience relatively large shifts for all protons except H2, H6, and H9. The abrupt change in chemical shifts may be caused by a sharp change in the environment around the protons of surfactant at

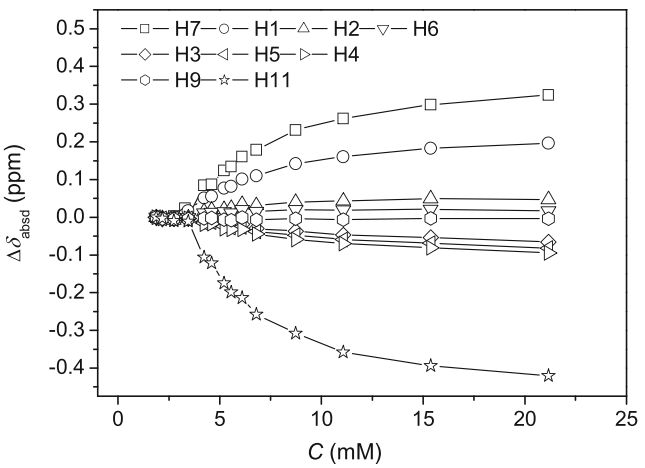

Fig. 7 Dependence of proton chemical shifts of [C_{12}iQuin]Br on ILs concentration in D_2O at 298 K

the CMC. The orientation of both aromatic ring and alkyl chain is analyzed in the following section.

It is well-known that the formation of H-bond causes the downfield shift, and ring parallel stacking leads to an upfield shift upon aggregation of SAILs containing aromatic rings in aqueous solutions [25]. Hence, the difference in the magnitude of chemical shift must be due to the difference ability of hydrogen bond formation and also of π–π interaction. The protons of H1 and H7 in the isoquinoline ring exhibit more acidity due to the proximity of electronegative nitrogen atoms and thereby their own availability to form hydrogen bonding. The significant downfield shift is observed in aqueous solutions of [C_{12}iQuin]Br above the CMC (Fig. 6a). This behavior can be justified by considering the effect of competing interactions Br^- and with water with H1 and H7 [39] because the Br^- is a stronger hydrogen-bond acceptor.

Nevertheless, an upfield shift of protons H1 and H7 in the chemical shift is observed with the increase of concentration in the case [C_4iQuin]Br and [C_8iQuin]Br (Fig. 6b, c; Table S1). The concentration of Br^- absorbing on the [C_{12}iQuin]Br micellar interface is much higher than that of [C_8iQuin]Br and [C_4iQuin]Br obtained by conductivity measurements; consequently, the ability of hydrogen bonding between H1, H7, and Br^- in [C_{12}iQuin]Br aggregate is stranger than that of [C_8iQuin]Br and [C_4iQuin]Br.

Previous work [40] has indicated that N-heterocyclic aromatic rings tend to stack, as the aromatic protons of a molecule experience the aromatic ring current effect from other nearby molecules. In the [C_{12}iQuin]Br micelle, isoquinoline ring stacking has been justified by the shift upfield of ^{1}H resonances of the H3, H4, and H5 protons and by the correlation peaks observed in the 2D NOESY spectra arising from adjacent protons (inter-proton distance usually within 0.5 nm). The 2D NOESY spectra of [C_{12}iQuin]Br in D_2O at concentrations of 2.5 mM (<CMC) and 30 mM (>CMC) are shown in Figs. S2 and 8, respectively. In contrast to the results from a dilute solution, additional correlation peaks (H1–H2, H2–H3, H6–H4, and H5–H4) were observed which confirmed the formation [C_{12}iQuin]Br micelle. This shows that the interactions between these proton pairs in the neighboring isoquinoline ring become strong enough to give rise to a significant NOE. The corresponding cross-signal intensities of the H7–H6 and H2–H3 are 11.01 and 8.73, respectively. The ratio of the distances of the proton pairs $r_{H7–H6}$ and $r_{H2–H3}$ is approximately 1.07 according to the literature method [41]. Taking into account isoquinoline's rigid bicyclic ring structure, the most likely conformer of adjacent isoquinolines is parallel stacking through the π–π interactions. This conclusion is correspondent with the reported results obtained using Møller–Plesset second-order perturbation theory along with the GIAO method for quinoline system [42]. In addition, protons H1 and

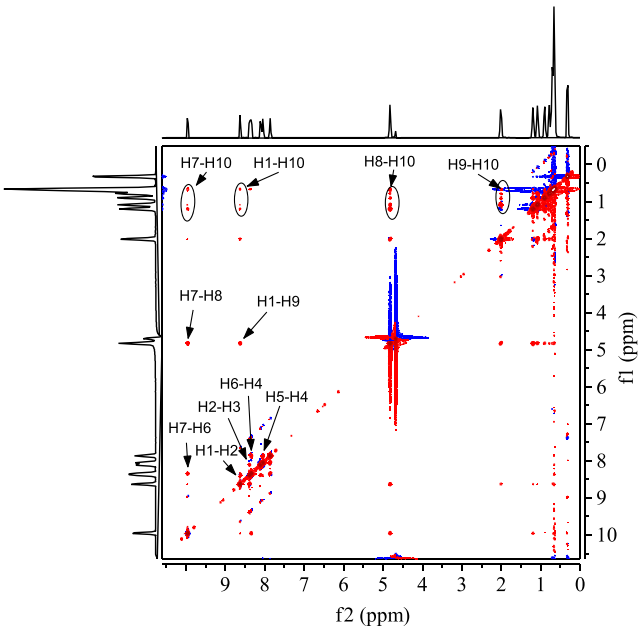

Fig. 8 2D NOESY spectra of [C_{12}iQuin]Br (30 mM) in D_2O at 298 K

H7 show relatively weaker shielding compared to others, which can be understood from the availability to form hydrogen bonding.

Even more interestingly, the resonance peaks of H2 and H6 multiplets move to downfield slightly and split into two clear doublets gradually with the increase in [C_{12}iQuin]Br concentration above the CMC (Fig. 6a). A plausible explanation for the observed peak splitting of H2 and H6 is that H2 lies in a more polar environment than H6 in the [C_{12}iQuin]Br micelle, which means the folding of the aromatic moiety toward the micellar core.

In the following section, we mainly focus on the chemical shift values of alkyl chain protons including the H8 and middle methylene groups (H10). The nature of the peak of H8 proton provides important information on the involvement of the counterions in the micellization. The downfield shift of the H8 proton for [C_{12}iQuin]Br molecule upon aggregation is

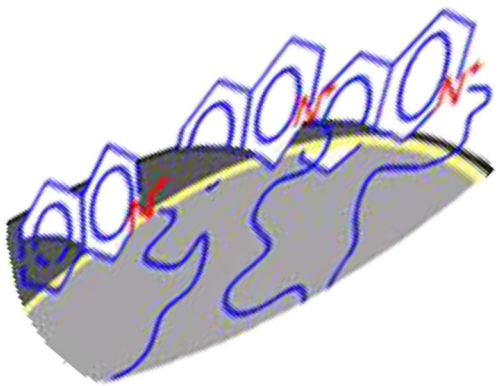

Fig. 9 Schematic representation of the structure of the [C_{12}iQuin]Br micelle

shown in Fig. 6a, which reveals that H-bond between the H8 and Br^- is present upon aggregation of [C_{12}iQuin]Br. As for [C_4iQuin]Br and [C_8iQuin]Br with shorter alkyl chain, the upfield shift of H8 proton is observed as shown in Fig. 6b, c, indicating that the contribution of H-bond is much weaker than the case of [C_{12}iQuin]Br due to lower local concentration between head group of [C_niQuin] and Br.

Interestingly, for [C_{12}iQuin]Br, the ^{1}H NMR spectrum of H10 shows two large multiplets and a small shoulder multiplet below the CMC. However, those peaks split into well-defined peaks at upfield above the CMC. The similar phenomenon was not observed in the [C_4iQuin]Br and [C_8iQuin]Br and [C_{12}Pyr]Br (not shown). However, the results of peaks split were observed in the 3-methyl-1-octylimidazolium chloride [C_8mim]Cl [25] and amphiphilic lauryl esters of L-phenylalanine aqueous solutions [43] because of the folding of aromatic moieties to the micellar core. Based on the examples mentioned above, the main effect factors of peak split can be drawn. The ^{1}H chemical shift of IL alkyl chain canting toward an aromatic head group upon aggregation in aqueous solution is mainly affected by the (1) transition of hydrophobic chains from water to the more hydrophobic core of the micelle leading to a decrease in the polarity of the microenvironment and a consequent downfield shift of the chain protons [44]; (2) micelle-induced changes of the conformation of the surfactant hydrophobic chain as from gauche to trans [45], which usually makes the protons in the middle of the alkyl chain shift downfield; and (3) diamagnetic anisotropy of the π–π conjugated system by the aromatic ring results in an unusual shielding of the methylene groups and thus to an upfield shift of their protons [46]. In all, micellization is expected to lead to a downfield shift, provided that the contribution of other shielding/deshielding mechanisms, such as from the surfactant head group (if anisotropic), are not dominant [47]. The cross peak between the protons H7 and H10 as well as between those of H1–H10 shown in the 2D NOESY spectra (Fig. 8) suggests that the CH_2 groups in the middle part of the alkyl chain would have an opportunity to be close to the H1 and H7 due to some of these chains being forced to bend and curve back [43, 48]. One can safely conclude that the packing of the aromatic ring and aliphatic chain of [C_{12}iQuin]Br is in proximity to each other within the micelle. The aromatic moieties are folding to the micellar core. Accordingly, the shielding of H10 protons shown in Fig. 6a could arise mainly from the effect of the aromatic ring current. One can also further infer that the difference in the position of the alkyl chain with respect to the isoquinoline ring leads to different shielding effects on CH_2 groups in the middle part of the alkyl chain, and thus, upfield shifts of the H10 in various changes of chemical shifts [49] and peak splitting were observed. Although the results for NMR measurements above indicate the orientation of aromatic ring in the [C_{12}iQuin]Br micelle, it is not possible to say with quite high confidence the morphology of micelle in aqueous solutions. Here, a partial schematic model of [C_{12}iQuin]Br micelle is shown in Fig. 9.

Conclusions

The micellization behavior of lauryl isoquinolinium bromide ([C_{12}iQuin]Br) in aqueous solution has been investigated using various techniques. The surface activity as well as the tendency of self-aggregate were demonstrated to be higher compared with the parent [C_{12}Pyr]Br and short-chain [C_n-iQuin]Br (n=4, 8). The charged phase separation model of micellization has been applied to the conductivity of [C_{12}iQuin]Br aqueous solutions, and it was found that the enthalpy and entropy of micellization for [C_{12}iQuin]Br are strongly temperature-dependent and compensate with each other. Compared with [C_{12}Pyr]Br, the values of enthalpy change at a specific temperature, ΔH^*_{mic}, is small. It is believed that this variation is due to the dramatic difference in the degree of aromatic rings stack between the isoquinoline ring and pyridine ring as determined by further NMR analysis. The aromatic moieties fold to the micellar core and stack parallelly through the π–π interactions of adjacent isoquinoline rings on the micellar interface.

Acknowledgments This work was financially supported by the National Nature Science Foundation of China (nos. 21073156 and 21203162) and project funded by the Priority Academic Program Development of Jiangsu Higher Education Institutions and Testing Center of Yangzhou University.

References

1. Tariq M, Freire MG, Saramago B, Coutinho JAP, Lopes JNC, Rebelo LPN (2012) Surface tension of ionic liquids and ionic liquid solutions. Chem Soc Rev 41:829–868
2. Blesic M, Marques MH, Plechkova NV, Seddon KR, Rebelo LPN, Lopes A (2007) Self-aggregation of ionic liquids: micelle formation in aqueous solution. Green Chem 9:481–4902
3. Ao MQ, Xu GY, Kang WL, Meng LW, Zhou T (2011) Surface rheological behavior of gelatin/ionic liquid-type imidazolium gemini surfactant mixed systems. Soft Matter 7:1199–1206
4. El Seoud OA, Pires PAR, Abdel-Moghny T (2007) Synthesis and micellar properties of surface-active ionic liquids: 1-alkyl-3-methylimidazolium chlorides. J Colloid Interface Sci 313:296–304
5. Galgano PD, El Seoud OA (2010) Micellar properties of surface active ionic liquids: a comparison of 1-hexadecyl-3-methylimidazolium chloride with structurally related cationic surfactants. J Colloid Interface Sci 345:1–11
6. Galgano PD, El Seoud OA (2011) Surface active ionic liquids: study of the micellar properties of 1-(1-alkyl)-3-methylimidazolium chlorides and comparison with structurally related surfactants. J Colloid Interface Sci 361:186–194
7. Shi LJ, Zheng LQ (2012) Aggregation behavior of surface active imidazolium ionic liquids in ethylammonium nitrate: effect of alkyl chain length, cations, and counterions. J Phys Chem B 116:2162–2172

8. Bowers J, Butts CP, Martin PJ, Vergara-Gutierrez MC, Heenan RK (2004) Aggregation behavior of aqueous solutions of ionic liquids. Langmuir 20:2191–2219
9. Chhatre AS, Joshi RA, Kulkarni BD (1993) Microemulsions as media for organic synthesis: selective nitration of phenol to ortho-nitrophenol using dilute nitric acid. J Colloid Interface Sci 158:183–187
10. Holmberg K (2003) Organic reactions in microemulsions. Curr Opin Colloid Interface Sci 8:187–196
11. Merritt MV, Chang IW, Flannery CA, Hsieh SJ, Lee K, Yung J (1995) Micelle-induced changes in the solvation of carbocations: effect of sodium dodecyl sulfate micelles on the enantiomer-specific oxygen exchange reactions of 1-phenyl-1-ethanol and 1-phenyl-1-butanol. J Am Chem Soc 117:9791–9799
12. Cornellas A, Perez L, Comelles F, Ribosa I, Manresa A, Garcia MT (2011) Self-aggregation and antimicrobial activity of imidazolium and pyridinium based ionic liquids in aqueous solution. J Colloid Interface Sci 355:164–171
13. Bandres I, Meler S, Giner B, Cea P, Lafuente C (2009) Aggregation behavior of pyridinium-based ionic liquids in aqueous solution. J Solut Chem 38:1622–1634
14. Jiang Z, Li XF, Yang GF, Cheng L, Yang Y (2012) pH-responsive surface activity and solubilization with novel pyrrolidone-based gemini surfactants. Langmuir 28:7174–7181
15. Sastry NV, Vaghela NM, Macwan PM, Soni SS, Aswal VK, Gibaud A (2012) Aggregation behavior of pyridinium based ionic liquids in water–surface tension, ^{1}H NMR chemical shifts, SANS and SAXS measurements. J Colloid Interface Sci 371:52–61
16. Dabholkar VV, Tripathi DR (2011) Synthesis and antibacterial activity of isochromene and isoquinoline derivative. J Heterocycl Chem 48:529–532
17. Lava K, Evrard Y, Van Hecke K, Van Meervelt L, Binnemans K (2012) Quinolinium and isoquinolinium ionic liquid crystals. RSC Adv 2:8061–8070
18. Visser AE, Holbrey JD, Rogers RD (2001) Hydrophobic ionic liquids incorporating *N*-alkylisoquinolinium cations and their utilization in liquid–liquid separations. Chem Commun 2001:2484–2485
19. Domańska U, Zawadzki M, Paduszyński K, Królikowski M (2012) Perturbed-chain SAFT as a versatile tool for thermodynamic modeling of binary mixtures containing isoquinolinium ionic liquids. J Phys Chem B 116:8191–8200
20. Domańska U, Zawadzki M, Lewandrowska A (2012) Effect of temperature and composition on the density, viscosity, surface tension, and thermodynamic properties of binary mixtures of *N*-octylisoquinolinium bis{(trifluoromethyl)sulfonyl}imide with alcohols. J Chem Thermodyn 48:101–111
21. Domańska U, Zawadzki M, Królikowska M, Tshibangu MM, Ramjugernath D, Letcher TM (2011) Measurements of activity coefficients at infinite dilution of organic compounds and water in isoquinolinium-based ionic liquid [C_8iQuin][NTf_2] using GLC. J Chem Thermodyn 43:499–504
22. Domańska U, Zawadzki M, Królikowski M, Lewandrowska A (2012) Phase equilibria study of binary and ternary mixtures of {*N*-octylisoquinolinium bis{(trifluoromethyl)sulfonyl}imide + hydrocarbon, or an alcohol, r water}. J Chem Thermodyn 181:63–71
23. Jaycock MJ, Parfitt GD (1981) Chemistry of interfaces. Wiley, New York, p 26
24. Filippov A, Shah FU, Glavatskih S, Antzutkin ON (2013) NMR self-diffusion study of a phosphonium bis(mandelato)borate ionic liquid. Phys Chem Chem Phys 15:9281–9287
25. Singh T, Kumar A (2007) Aggregation behavior of ionic liquids in aqueous solutions: effect of alkyl chain length, cations, and anions. J Phys Chem B 111:7843–7851
26. Zhao Y, Gao SJ, Wang JJ, Tang JM (2008) Aggregation of ionic liquids [Cnmim]Br (*n*=4, 6, 8, 10, 12) in D2O: a NMR study. J Phys Chem B 112:2031–2039
27. Huang X, Han YH, Wang YX, Wang YL (2007) Aggregation behavior of nitrophenoxy-tailed quaternary ammonium surfactants. J Phys Chem B 111:12439–12446
28. Rosen MJ (1989) Surfactants and interfacial phenomena, 2nd edn. Wiley, New York
29. Shi LJ, Li N, Yan H, Gao YA, Zheng LQ (2011) Aggregation behavior of long-chain *N*-aryl imidazolium bromide in aqueous solution. Langmuir 27:1618–1625
30. Shanks PC, Franses EI (1992) Estimation of micellization parameters of aqueous sodium dodecyl sulfate from conductivity data. J Phys Chem 96:1794–1805
31. Wadekar MN, Boekhoven J, Jager WF, Koper GJM, Picken SJ (2012) Micellization behavior of aromatic moiety bearing hybrid fluorocarbon sulfonate surfactants. Langmuir 28:3397–3402
32. Shi LJ, Li N, Zheng LQ (2011) Aggregation behavior of long-chain *N*-aryl imidazolium bromide in a room temperature ionic liquid. J Phys Chem C 115:18295–18301
33. Sugihara G, Hisatomi M (1999) Enthalpy–entropy compensation phenomenon observed for different surfactants in aqueous solution. J Colloid Interface Sci 219:31–36
34. Chen LJ, Lin SY, Huang CC (1998) Effect of hydrophobic chain length of surfactants on enthalpy–entropy compensation of micellization. J Phys Chem B 102:4350–4356
35. Galan JJ, Rodrıguez JR (2010) Thermodynamic study of the process of micellization of long chain alkyl pyridinium salts in aqueous solution. J Therm Anal Calorim 101:359–364
36. Lehanine Z, Badache L (2011) Thermodynamics of micellization of cationic surfactants based on *O*-alkyl and *O*-perfluoro-*N*, *N*′-diisopropylisourea: effect of the counter ion nature. J Chem Thermodyn 43:1342–1348
37. Perger TM, Bester-Rogac M (2007) Thermodynamics of micelle formation of alkyltrimethylammonium chlorides from high performance electric conductivity measurements. J Colloid Interface Sci 313:288–295
38. Galan J, Gonzalez-Perez A, Del Castillo JL, Rodriguez JR (2002) Thermal parameters associated to micellization of dodecylpyridinium bromide and chloride in aqueous solution. J Therm Anal Calorim 70:229–234
39. Headley AD, Kotti SRSS, Nam J, Li KY (2005) Effect of hydrophobic side-chains on the solvation of imidazolium salts. J Phys Org Chem 18:1018–1022
40. Guin M, Patwari GN, Karthikeyan S, Kim KS (2011) Do N-heterocyclic aromatic rings prefer π-stacking? Phys Chem Chem Phys 13:5514–5525
41. Yang XY, Gao HC, Du YR et al (2004) Difference in micellar properties of sodium dodecyl sulfonate from sodium 4-decyl naphthalene sulfonate in D_2O solution studied by ^{1}H NMR relaxation and 2D NOESY. Colloid Polym Sci 282:280–286
42. Majumder M, Sathyamurthy N (2012) A theoretical investigation on the effect of π–π stacking interaction on ^{1}H isotropic chemical shielding in certain homo- and hetero-nuclear aromatic systems. Theor Chem Accounts 131:1092
43. Vijay R, Mandal AB, Baskar G (2010) ^{1}H NMR spectroscopic investigations on the conformation of amphiphilic aromatic amino acid derivatives in solution: effect of chemical architecture of amphiphiles and polarity of solvent medium. J Phys Chem B 114:13691–13702
44. Tada EB, Novaki LP, El Seoud OA (2001) Solvatochromism in cationic micellar solutions: effects of the molecular structures of the solvatochromic probe and the surfactant headgroup. Langmuir 17:652–658
45. Okano LT, El Seoud OA, Halstead TK (1997) A proton NMR study on aggregation of cationic surfactants in water: effects of the structure of the headgroup. Colloid Polym Sci 274:138–145

46. Dong B, Gao YA, Su YJ, Zheng LQ, Xu JK, Inoue T (2010) Self-aggregation behavior of fluorescent carbazole-tailed imidazolium ionic liquids in aqueous solutions. J Phys Chem B 114:340–348
47. Shimizu S, El Seoud OA (2003) Synthesis and aggregation of benzyl (2-acylaminoethyl) dimethylammonium chloride surfactants. Langmuir 19:238–243
48. Zhao J, Fung BM (1993) Conformation change of hydrocarbon chains upon the formation of micelle. J Phys Chem 97:5185–5187
49. Suratkar V, Mahapatra S (2000) Solubilization site of organic perfume molecules in sodium dodecyl, sulfate micelles: new insights from proton NMR studies. J Colloid Interface Sci 225:32–38